

Saturation of number variance in embedded random matrix ensembles

Ravi Prakash* and Akhilesh Pandey†

School of Physical Sciences, Jawaharlal Nehru University, New Delhi – 110067, India

We study fluctuation properties of embedded random matrix ensembles of non-interacting particles. For ensemble of two non-interacting particle systems, we find that unlike the spectra of classical random matrices, correlation functions are non-stationary. In the locally stationary region of spectra, we study the number variance and the spacing distributions. The spacing distributions follow the Poisson statistics which is a key behavior of uncorrelated spectra. The number variance varies linearly as in the Poisson case for short correlation lengths but a kind of regularization occurs for large correlation lengths, and the number variance approaches saturation values. These results are known in the study of integrable systems but are being demonstrated for the first time in random matrix theory. We conjecture that the interacting particle cases, which exhibit the characteristics of classical random matrices for short correlation lengths, will also show saturation effects for large correlation lengths.

PACS numbers: 05.45.Mt, 24.60.Ky, 05.40.-a

I. INTRODUCTION

Random matrix theory has become a great tool to study energy level statistics of quantum chaotic systems, such as complex nuclei, mesoscopic transport, Sinai billiard, etc [1–11]. It is also applicable to time series problems [12–14], communication theory [15, 16] etc. The local level fluctuations are universal and depend only on the symmetry class of the system. It is conjectured and confirmed by numerical and experimental results that quantum chaotic systems follow Wigner repulsion whereas integrable systems exhibit Poisson statistics [17–20].

Although random matrix theories successfully describe many universal properties, they are valid only for short correlation lengths with respect to the size of the spectra. The number variance statistic, $\Sigma^2(r)$, exhibits logarithmic and linear behavior at such correlation lengths for quantum chaotic and integrable systems respectively; here $\Sigma^2(r)$ is the variance of the number of levels in intervals of length rD , where D is the local average spacing.

A numerical analysis of the spectrum of quantum rectangular billiard shows that while $\Sigma^2(r)$ starts linearly for small r as in the Poisson case, it eventually becomes a constant [21]. Berry [20] has shown by semi-classical methods that this is a generic behavior of quantum integrable systems. He has also predicted that a similar saturation effect will be seen in the spectra of quantum chaotic systems. Thus the saturation phenomenon is universal for real quantum systems, but the saturation value varies from system to system. We also mention that the saturation phenomenon has been found for the Riemann- ζ function [22, 23].

It is believed that the saturation phenomenon will not be seen in random matrix ensembles. This is certainly true for the Gaussian, circular and other related invariant

ensembles. Our purpose in this article is to show that the embedded ensembles (EE) [2, 24–28] exhibit saturation effects. Embedded ensembles are ensembles of m -particle systems with interactions of rank k (i.e., k -particle interactions), where $k < m$. These are applicable to the study of statistical properties of many particle systems. We mention that the saturation phenomenon in embedded ensemble has been predicted [29], but has never been verified. This conjecture was based on the observation that very short wavelength fluctuations in the embedded ensembles are suppressed [27, 30].

In this article, we consider the embedded random matrix ensemble of two non-interacting particles, i.e., $k = 1$ and $m = 2$. We derive expressions for the spectral density and the two-level correlation function and show that the level fluctuation statistics are non-stationary. We also confirm that the very short wavelength fluctuations are indeed suppressed. We study the number variance statistics which display linear behavior for short correlation lengths, as it should for integrable systems, but approaches saturation as we go towards higher lengths, confirming thereby the above mentioned conjecture. We believe that the saturation will also be found in the interacting case, but this is difficult to demonstrate.

This article is organized as follows. In section II, we describe the EEs of non-interacting particles and their n -level correlation functions. We derive expressions for the spectral density and the two-level correlation function in sections III and IV respectively. These expressions are required for the unfolding of the spectrum and the evaluation of the number variance as well as the spacing distribution. In section V, we study the spectral form factor and the number variance. The numerical method to study the form factor and the number variance is discussed in section VI. The short-range behavior is studied in terms of nearest neighbor spacing distributions as well as number variance and is discussed in section VII. The saturation phenomenon at large correlation lengths is discussed in section VIII. In sections IX, X, XI, we obtain the number variance and their satu-

* raviprakash.sps@gmail.com

† ap0700@mail.jnu.ac.in; apandey2006@gmail.com

ration values for the unitary, symplectic and orthogonal cases of EEs respectively. In these sections we have taken 1000-dimensional one-particle spectra with constant average density. To improve the statistics significantly we consider 5000-dimensional one-particle spectra in section [XII](#). In section [XIII](#), we consider an example of non-uniform average density. We summarize our results in section [XIV](#). In Appendices [A-E](#), some details of the analytical calculations are given.

II. EMBEDDED RANDOM MATRIX ENSEMBLES

For a system of m non-interacting fermions, the energy levels can be defined as,

$$E = \sum n_j \epsilon_j, \quad (1)$$

where the ϵ_j are the single particle energy levels and the n_j are occupancy numbers with values 0, 1 such that $\sum n_j = m$. The boson case can also be considered similarly. The single particle Hamiltonian is modeled by Gaussian ensemble. We consider all three types viz., Gaussian orthogonal (GOE), Gaussian unitary (GUE) and Gaussian symplectic (GSE) ensembles. We shall refer to the corresponding embedded ensembles as non-interacting embedded GOE (EGOE), embedded GUE (EGUE) and embedded GSE (EGSE) respectively [[2](#), [27](#)]. There are N single particle energy levels. The dimension of the m -particle spectra will be,

$$d_m = \frac{N!}{m!(N-m)!}. \quad (2)$$

Thus for two particles, it will be $d_2 = N(N-1)/2$.

Let $P(x_1, \dots, x_N)$ be the joint probability distribution (jpd) of the single-particle levels. Then the one-particle n -level correlation function, $R_n(x_1, \dots, x_n)$ is defined by

$$R_n = \frac{N!}{(N-n)!} \int \dots \int P(x_1, \dots, x_N) dx_{n+1} \dots dx_N. \quad (3)$$

The m -particle correlation functions have similar definitions with N replaced by d_m .

We write correlation functions in terms of cluster functions. The n -level correlations, R_n can be written in terms of cluster function T_n as follows [[3](#), [31](#)]

$$R_n = \sum_G (-1)^{n-q} \prod_{j=1}^q T_{G_j}(x_k, \text{with } k \text{ in } G_j), \quad (4)$$

where G stands for any division of the indices $(1, \dots, n)$ into q subgroups (G_1, \dots, G_q) . For example, the one and two-level correlation functions can be written as,

$$R_1(x) = T_1(x) \quad (5)$$

and

$$R_2(x_1, x_2) = T_1(x_1)T_1(x_2) - T_2(x_1, x_2). \quad (6)$$

Since we are dealing with non-interacting particles, the n -level correlation function for the two-particle spectra can be written in terms of one-particle p -level correlation functions, where $p \leq 2n$. We denote the one-particle and two-particle correlation functions by R_n and $R_n^{(2)}$ respectively. A similar convention will also be used for other physical quantities unless or otherwise stated explicitly.

We write correlation functions for single particle spectrum in terms of cluster functions. The detailed derivation is provided in Appendix [A](#). We get following expressions for spectral density and two-level correlation function for two-particle spectrum,

$$R_1^{(2)}(\xi) = \frac{1}{2} \int_{-\infty}^{\infty} \int_{-\infty}^{\infty} [T_1(x_1)T_1(x_2) - T_2(x_1, x_2)] \times \delta(\xi - (x_1 + x_2)) dx_1 dx_2. \quad (7)$$

The two-level correlation function is given by,

$$R_2^{(2)}(\xi_1, \xi_2) = \int_{-\infty}^{\infty} \int_{-\infty}^{\infty} \int_{-\infty}^{\infty} \int_{-\infty}^{\infty} \left[\frac{1}{4} R_4(x_1, x_2, x_3, x_4) + R_3(x_1, x_2, x_3) \delta(x_1 - x_4) \right] \delta(\xi_1 - (x_1 + x_2)) \times \delta(\xi_2 - (x_3 + x_4)) dx_1 dx_2 dx_3 dx_4. \quad (8)$$

R_2 and R_1 terms do not appear in [\(8\)](#) because we are dealing with fermions. The expression can also be written in terms of cluster functions by substituting [\(A1\)](#) and [\(A2\)](#) in [\(8\)](#).

III. SPECTRAL DENSITY FOR THE TWO-PARTICLE SPECTRUM

We consider single particle spectrum as unfolded spectrum so that the average spectral density is uniform ([Fig.1a](#)). The non-uniform case is briefly discussed in the section [XIII](#). The average density, R_1 , is taken as,

$$R_1(x) = \begin{cases} 1, & -\frac{N}{2} \leq x \leq \frac{N}{2}, \\ 0, & \text{otherwise.} \end{cases} \quad (9)$$

For the Gaussian ensembles mentioned above, the correlation and the cluster functions are translationally invariant, and therefore, T_2 is a function of the difference of its arguments [[32](#)]. We, therefore, introduce new cluster function Y_2 for the unfolded spectrum,

$$Y_2(x_1 - x_2) = T_2(x_1, x_2). \quad (10)$$

By using [\(10\)](#), the two-particle spectral density given in [\(7\)](#) can be written as,

$$R_1^{(2)}(\xi) = \frac{1}{2} \int_{-N/2}^{N/2} \int_{-N/2}^{N/2} [T_1(x_1)T_1(x_2) - Y_2(x_1 - x_2)] \times \delta(\xi - (x_1 + x_2)) dx_1 dx_2. \quad (11)$$

Integral of the first term is the convolution of T_2 with itself. Integration of the second term depends on the

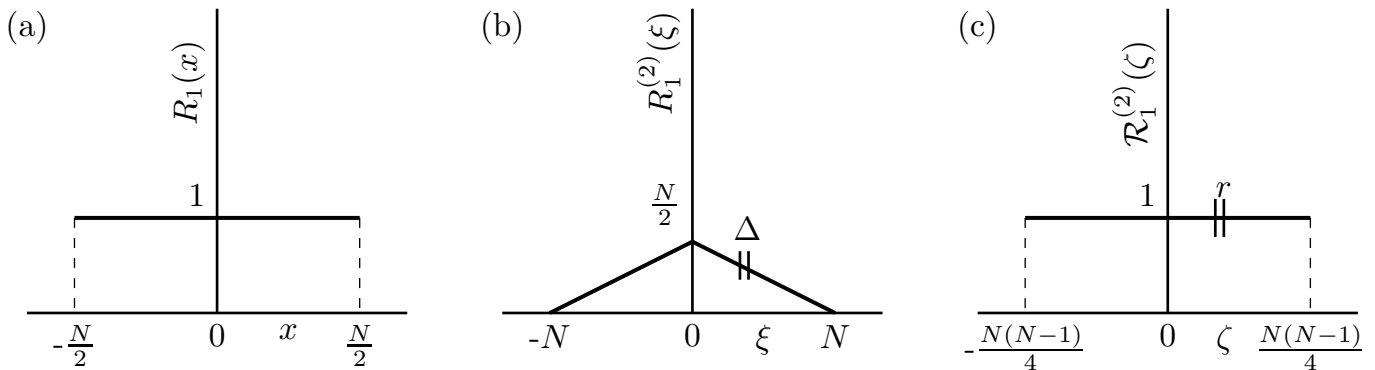


FIG. 1. Schematic representation of (a) Spectral density for an unfolded one-particle spectrum, (b) Spectral density for corresponding two-particle spectrum and (c) Spectral density for the unfolded two-particle spectrum.

ensemble. However in the large N limit and away from the end of the spectrum ($|\xi| < N$), this integral is equal to half of the normalization of Y_2 . Substituting (9) in (11), we get,

$$R_1^{(2)}(\xi) = \begin{cases} \frac{N}{2} - \frac{|\xi|}{2} - \frac{1}{4}, & -N \leq \xi \leq N, \\ 0, & \text{otherwise.} \end{cases} \quad (12)$$

Above expression describes the spectral density for two particle system (Fig.1b). For large N , the last term (i.e., $-1/4$) can be dropped. We will use this approximation to unfold the two-particle spectrum.

IV. TWO-LEVEL CORRELATION FUNCTION FOR THE TWO-PARTICLE SPECTRUM

The two-level correlation function for the two-particle spectrum given in (8) can be simplified considerably for large N . See Appendix B for detailed calculation. We find that the two-level cluster function is given by,

$$T_2^{(2)}(\xi_1, \xi_2) = \frac{N - |\xi|}{2} \left[2Y_2(\Delta) - \int_{-\infty}^{\infty} Y_2(x)Y_2(\Delta - x)dx \right], \quad (13)$$

where

$$\xi = \frac{\xi_1 + \xi_2}{2}, \quad \Delta = \xi_2 - \xi_1 \quad (14)$$

See Fig. 1 for ξ and Δ . We consider $|\Delta| = O(1)$, which means that the number of two-particle energy levels in $|\Delta|$ is $O(N)$.

To study the local fluctuations we unfold the two-particle spectrum by introducing the new variable ζ defined by,

$$\zeta = \int_0^\xi R_1^{(2)}(\xi') d\xi'. \quad (15)$$

The average spectral density, $\mathcal{R}_1^{(2)}(\zeta)$, in the new variable, ζ , is one (Fig.1c). The average number of level in

the interval $[\xi_1, \xi_2]$ is $|r|$, where r is given by,

$$r = \zeta_2 - \zeta_1 = R_1^{(2)}(\xi)\Delta. \quad (16)$$

The unfolded two-level cluster function is defined as,

$$Y_2^{(2)}(r; \xi) \equiv \frac{T_2^{(2)}(\xi_1, \xi_2)}{R_1^{(2)}(\xi_1)R_1^{(2)}(\xi_2)}. \quad (17)$$

$Y_2^{(2)}(r; \xi)$ is given in terms of the one-particle cluster function as,

$$Y_2^{(2)}(r; \xi) = \frac{1}{R_1^{(2)}(\xi)} \left[2Y_2(\Delta) - \int_{-\infty}^{\infty} Y_2(x)Y_2(\Delta - x) dx \right], \quad (18)$$

where Δ should be written in terms of r as in (16). The density in a localized region can be assumed to be constant and therefore $R_1^{(2)}(\xi_1) \approx R_1^{(2)}(\xi_2) \approx R_1^{(2)}(\xi)$. The cluster function, $Y_2^{(2)}(r; \xi)$ is non-stationary globally as it depends on ξ . Note that (18) holds only for uniform single-particle density. Our results given in sections V-XII are all for the uniform case. We consider the non-uniform case briefly in section XIII.

V. SPECTRAL FORM FACTOR AND NUMBER VARIANCE

The two-level form factor $b_2^{(2)}(k; \xi)$ (or the Fourier transform of $Y_2^{(2)}(r; \xi)$) [3, 33] for the two-particle system,

$$b_2^{(2)}(k; \xi) = \int_{-\infty}^{\infty} Y_2^{(2)}(s; \xi) e^{2\pi i k s} ds, \quad (19)$$

is of special interest, as it will help us express number variance in a compact form. It can be written in terms of one-particle form factor (i.e., the Fourier transform of $Y_2(s)$),

$$b_2(k) = \int_{-\infty}^{\infty} Y_2(s) e^{2\pi i k s} ds. \quad (20)$$

The Fourier transform of the first term in (18) gives $2b_2(kR_1^{(2)}(\xi))$. The second term is the convolution of Y_2 with itself. Therefore its Fourier transform yields $\left[b_2(kR_1^{(2)}(\xi))^2\right]$. Thus spectral form factor for the two-particle spectrum can be written as,

$$b_2^{(2)}(k; \xi) = 2b_2(kR_1^{(2)}(\xi)) - b_2(kR_1^{(2)}(\xi))^2. \quad (21)$$

Eqs.(18) and (21) connect the cluster function with one-particle cluster function.

It will be convenient to introduce the two-point form factor $F_2^{(2)}$ as,

$$F_2^{(2)}(k; \xi) = 1 - b_2^{(2)}(k; \xi) \quad (22)$$

which is the Fourier transform of the two-point correlation function, $S_2^{(2)}(r; \xi) = \delta(r) - Y_2^{(2)}(r; \xi)$, with $\delta(r)$ being the self-correlation term. Substituting in (21), we get,

$$\begin{aligned} F_2^{(2)}(k; \xi) &= \left[1 - b_2(kR_1^{(2)}(\xi))\right]^2 \\ &= \left[F_2(kR_1^{(2)}(\xi))\right]^2, \end{aligned} \quad (23)$$

where $F_2(k) = 1 - b_2(k)$ represents the Fourier transform of the two-point correlation function, $S(r)$, for the corresponding one-particle spectrum.

The variance $\Sigma^2(r; \xi)$ of the number of levels, n , in the interval $[\zeta_1, \zeta_2]$ with $\zeta_2 > \zeta_1$ is defined as,

$$\Sigma^2(r; \xi) = \overline{n^2} - \bar{n}^2, \quad (24)$$

where $r = \bar{n}$. The bar denotes the ensemble average. The number variance can be calculated from the two-level cluster function and is given by [2, 3],

$$\Sigma^2(r; \xi) = r - 2 \int_0^r (r-s) Y_2^{(2)}(s; \xi) ds. \quad (25)$$

It can also be written in terms of the two-point form factor as [34],

$$\Sigma^2(r; \xi) = \int_{-\infty}^{\infty} F_2^{(2)}(k; \xi) \left(\frac{\sin(\pi kr)}{\pi k}\right)^2 dk. \quad (26)$$

We will use the above expression for evaluating the number variance for the EEs.

VI. NUMERICAL STUDY

We construct the spectra of two non-interacting particle system numerically by using unfolded Gaussian ensemble spectra in (1). The one-particle spectra lie in the interval $[-N/2, N/2]$ with uniform average density. The spectral density for the two-particle system is a tent like

function in the interval $[-N, N]$ as shown in Fig.1b. We then unfold the two-particle spectra using the unfolding relation given in (15) so that the average spectral density is equal to 1 (Fig.1c). Since spectral correlations are non-stationary, we consider a part of the tent spectrum which is small enough so that the density does not vary significantly and also large enough to have approximately $O(N)$ levels. We verify in the later sections the two-particle form factor $F_2^{(2)}(k; \xi)$ and number variance for all three embedded ensembles discussed in Section II.

To calculate the form factor, $F_2^{(2)}(k; \xi)$ function, we consider the level correlation in the Fourier space. The two-level form factor can be written as,

$$F_2^{(2)}(k; \xi) = \frac{1}{N} \left[\left| \sum_j e^{2\pi i k \zeta_j} \right|^2 - \left| \sum_j e^{2\pi i k \zeta_j} \right|^2 \right], \quad (27)$$

where the ζ_j are levels of the unfolded spectra. We numerically evaluate the right-hand side for spectra under consideration. The expression can be verified analytically by evaluating the sum on the right-hand side in the continuum limit. The number variance is calculated by using (24).

In this article, our numerical samples consist of ensembles having 100000 spectra of the two-particle system. The spectra are constructed from all three types of Gaussian ensembles, each of dimension $N = 1000$. We have done calculations for three different regions of the spectra denoted by $\xi = 3.0, 105.6$ and 225.5 . These values correspond to $\zeta = 1500, 50000$ and 100000 respectively in the corresponding unfolded spectra. We have also considered matrices with $N = 5000$ but with a smaller ensemble having 5000 spectra in each case and $\xi = 20.0$ (with $\zeta = 50000$).

VII. SHORT RANGE BEHAVIOR

The two-particle spectrum is constructed by addition of energy levels of one particle spectrum. The eigenvalues exhibit the characteristics of uncorrelated spectrum. Therefore spectra of non-interacting particles should display the Poisson statistics for small correlation lengths - a characteristic of integrable systems. We first consider the number variance to illustrate the short range behavior. From (23, 26) one can predict that for short correlation lengths, viz. $r \ll N$, Poisson behavior will be obtained. The one-particle form factor $F_2(k)$ for the Gaussian ensembles increases from zero and goes to one for $|k| \gtrsim 1$. Eq. (23) implies that for two-particle spectra $F_2^{(2)}(k; \xi)$ is one for $kR_1^{(2)} \gtrsim 1$ or $k \gtrsim 1/N$ because the spectral density for the two-particle spectra is of the order N . See Fig.6, Fig.8 and Fig.10 ahead. By substituting, $F_2^{(2)}(k; \xi) = 1$ in (26), we obtain the Poisson

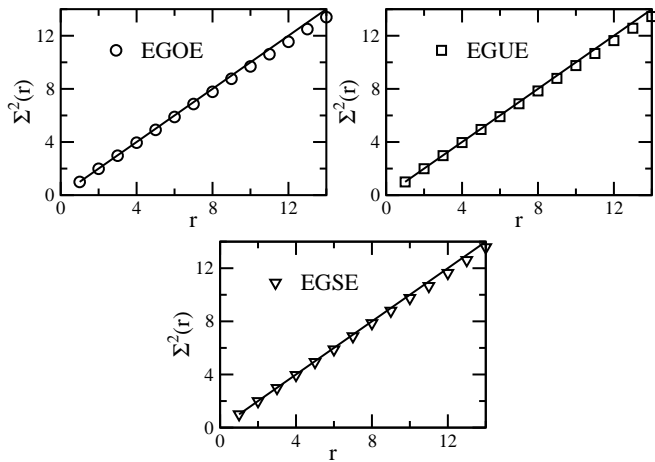


FIG. 2. Number variance at short correlation lengths for all three types of EEs. Agreement with Poisson result, shown by solid lines, is excellent.

result in the large N limit,

$$\begin{aligned} \Sigma^2(r; \xi) &= 2 \int_0^\infty \left(\frac{\sin(\pi kr)}{\pi k} \right)^2 dk \\ &= r. \end{aligned} \quad (28)$$

This is shown in Fig.2 for all three types of EEs.

Next we consider the nearest neighbor spacing distribution. The k^{th} -nearest neighbor spacing distribution $P_k(s)$ viz. the distribution of spacing between two levels with k levels in the middle, exhibits Poisson statistics. $P_k(s)$ for integrable systems is given by,

$$P_k(s) = \frac{s^k}{k!} e^{-s}. \quad (29)$$

Our results are shown in Fig.3 for all three types of EEs, viz., EGOE, EGUE and EGSE.

The agreement with the Poisson result is excellent for the number variance as well as the spacing distribution.

VIII. SATURATION PHENOMENON IN NUMBER VARIANCE

Saturation of number variance for large correlation lengths, $r \gtrsim N$, comes from the suppression of fluctuations of short-wave frequencies (or large wavelengths). To explain it, we consider a model where the fluctuations of frequencies $< \delta$ are completely absent. The two-point form factor is given by

$$\mathcal{F}_2(k) = \begin{cases} 0, & 0 \leq |k| \leq \delta, \\ 1, & \delta < |k| < \infty. \end{cases} \quad (30)$$

The number variance is evaluated using (26) for the above form factor and is shown in Fig.4 for several values of δ .

For $\delta = 0$, Poisson result is obtained. For $\delta > 0$, the number variance is Poisson-like for small r and approaches saturation value $1/(\pi^2\delta)$ for large r ; see (33) ahead.

For saturation to occur in the general case, (26) should converge for large values of r , i.e., $F_2^{(2)}(k; \xi) = O(|k|^\epsilon)$ for small $|k|$ with $\epsilon > 1$. The saturation value can now be evaluated by replacing $(\sin(\pi kr))^2$ in (26) by $1/2$, its average over r for large r . Thus, we have,

$$\Sigma_{\text{sat}}^2(r; \xi) = \int_{-\infty}^{\infty} F_2^{(2)}(k; \xi) \frac{1}{2\pi^2 k^2} dk. \quad (31)$$

This will be verified ahead for systems of two non-interacting particles in sections IX, X, XI for EGUE, EGOE and EGSE respectively by rigorous calculations. Note that the saturation does not apply to the Gaussian and Poisson ensembles because in these cases (31) is not convergent.

We also mention that the suppression of short wave frequencies should occur in the case of interacting embedded ensembles also [27, 30] and, therefore, we expect (31) to apply again. In these cases, it is known from numerical simulations that the short-range fluctuations are identical to those of Gaussian ensembles [26]. By generalizing (30), we can make a heuristic model for this case also. We consider the form factor

$$\mathcal{F}_2(k) = \begin{cases} 0, & 0 \leq |k| \leq \delta, \\ g(k), & \delta < |k| < \infty, \end{cases} \quad (32)$$

where $g(k) = 1 - b_2(k)$ is the form factor of the Gaussian ensembles. Using (31) we can predict that Σ^2 will become a constant for large r with value given by,

$$\Sigma_{\text{sat}}^2(r) = 2 \int_\delta^\infty \frac{g(k)}{2\pi^2 k^2} dk. \quad (33)$$

We show Σ^2 in Fig.5 using $g(k)$ of GOE, GUE and GSE, given ahead in (52), (36) and (44) respectively. For $\delta > 0$, the number variance shows good agreement with the Gaussian ensemble results for $r \lesssim 10$ for the values of δ chosen. For larger values of r , saturation is observed and is consistent with (33). We mention however that saturation in the interacting case has not yet been demonstrated in numerical simulations of embedded ensembles nor in the simulations of quantum chaotic systems. See however [22, 23] for saturation in the statistics of zeros of Riemann- ζ function.

In the earlier numerical and semiclassical calculations [20, 21] for integrable and chaotic spectra of two degrees of freedom, saturation has been studied in terms of the rigidity statistics $\overline{\Delta}_3(r)$. This is related to $\Sigma^2(r)$ by [32]

$$\overline{\Delta}_3(r) = \frac{2}{r^4} \int_0^r (r^3 - 2r^2 s + s^3) \Sigma^2(s) ds, \quad (34)$$

and therefore the corresponding saturation values are also related:

$$\overline{\Delta}_{3\text{sat}} = \frac{1}{2} \Sigma_{\text{sat}}^2. \quad (35)$$

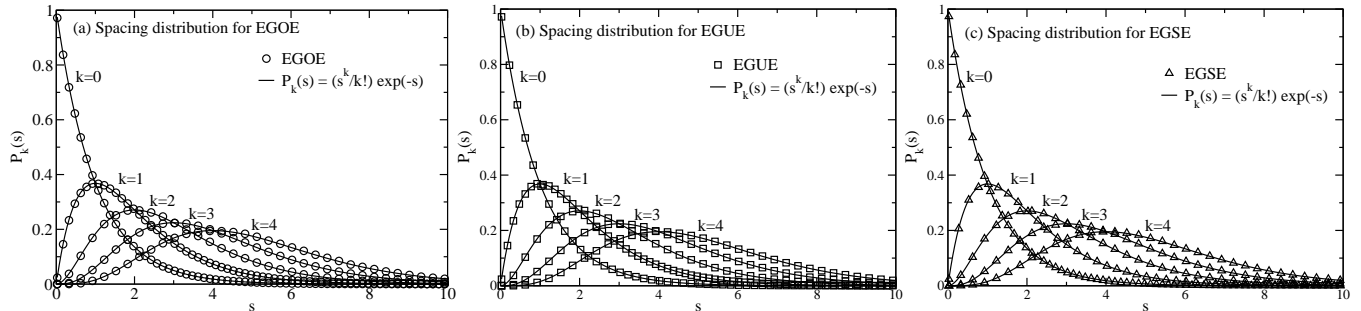


FIG. 3. k^{th} -nearest neighbor spacing distribution of twoth particle unfolded spectra. $k = 0$ denotes the nearest neighbor spacing distribution. Solid lines show the theoretical results for the normalized Poisson distribution.

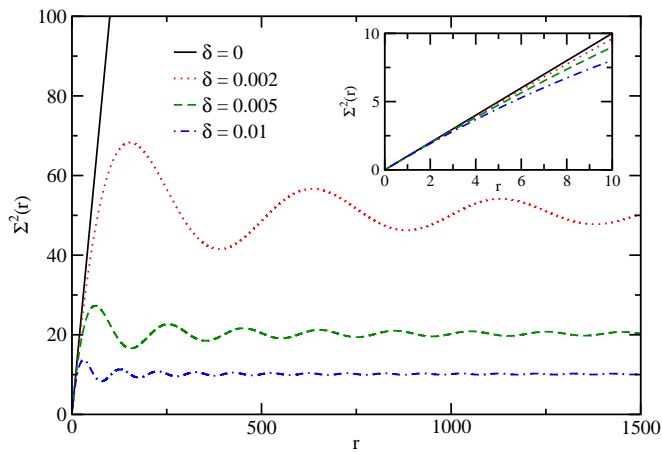


FIG. 4. (Color online) The number variance for the form factor given in (30) for several values of δ . Inset shows the same figure for small correlation lengths.

IX. EMBEDDED GAUSSIAN UNITARY ENSEMBLE

We start with the simplest case, i.e., the EGUE. The form factor for the single particle spectrum is given by [3],

$$b_2(k) = \begin{cases} 1 - |k|, & |k| \leq 1, \\ 0, & |k| \geq 1. \end{cases} \quad (36)$$

Substituting this in the expression for the two-level form factor given in (23), we get,

$$F_2^{(2)}(k; \xi) = \begin{cases} \chi, & |\chi| \leq 1, \\ 1, & |\chi| > 1, \end{cases} \quad (37)$$

where $\chi = kR_1^{(2)}(\xi)$. We numerically calculate the form factor, $F_2^{(2)}(k; \xi)$ as discussed in Section VI. The form factor at several locations in the two-particle spectra denoted by ξ is shown in Fig. 6. The results are in excellent agreement with the analytical results given in (37) and confirm the suppression of correlations for short frequencies ($|k| = O(N)$).

For number variance, we substitute in (26) the expression for the form factor given in (37). See Appendix C for detailed calculation. We find,

$$\Sigma^2(r; \xi) = \frac{R_1^{(2)}(\xi)}{\pi^2} \left[2 + \pi^2 \Delta - \cos(2\pi\Delta) - \frac{\sin(2\pi\Delta)}{2\pi\Delta} - 2\pi\Delta \text{Si}(2\pi\Delta) \right], \quad (38)$$

where $\Delta = r/R_1^{(2)}(\xi)$ and Si is the sine-integral function, defined as,

$$\text{Si}(x) = \int_0^x \frac{\sin(s)}{s} ds. \quad (39)$$

Number variance, $\Sigma^2(r)$, is plotted against correlation length, r , in Fig. 7. The agreement is very good for $r \approx N$. The small rise in Σ^2 for larger values of r is due to finite size effect. We will see in Section XII that the results become much better for $N = 5000$.

To find the number variance for small values of r , one can make Taylor expansion of (38) around zero. The number variance for small values of r can be written as,

$$\Sigma^2(r; \xi) = R_1^{(2)}(\xi) \left[\Delta - \frac{4}{3} \Delta^2 + \dots \right]. \quad (40)$$

By using (16), we get,

$$\Sigma^2(r; \xi) = r - \frac{4}{3} \frac{1}{R_1^{(2)}(\xi)} r^2 + \dots \quad (41)$$

Since spectral density, $R_1^{(2)}(\xi)$, is $O(N)$, the number variance is linear for $r \ll N$, as verified in Fig. 2.

Number variance saturates at large correlation lengths, i.e., $r = O(N)$. We expand sine integral function given in (39) up to a few leading order terms,

$$\begin{aligned} \text{Si}(x) &= \frac{\pi}{2} - \int_x^\infty \frac{\sin(s)}{s} ds \\ &= \frac{\pi}{2} - \frac{\cos(x)}{x} - \frac{\sin(x)}{x^2} + O(x^{-3}). \end{aligned} \quad (42)$$

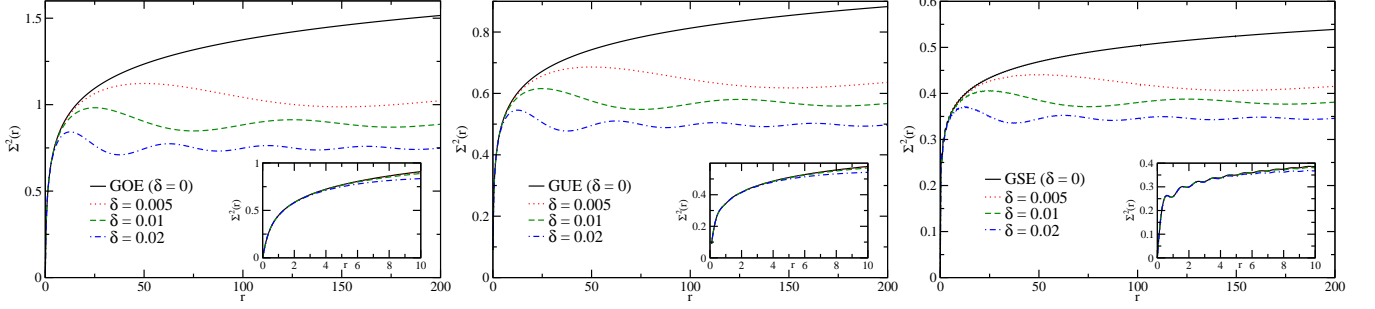


FIG. 5. (Color online) Number variance for the model for interacting particle system discussed in Section VIII for several values of δ . Inset of each Figure shows the corresponding short range behavior.

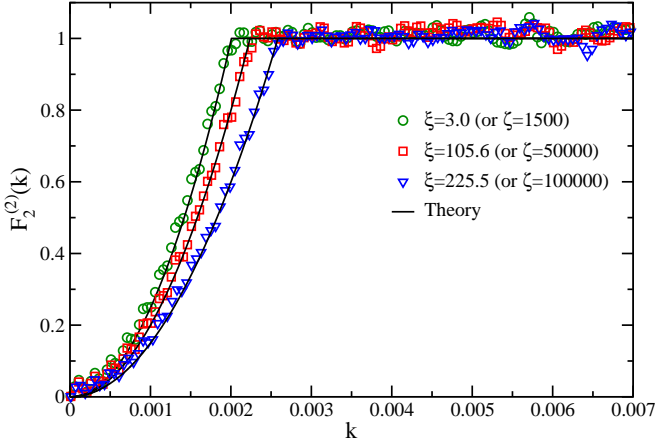


FIG. 6. (Color online) The two particle form factor for EGUE in different regions of spectra denoted by $\xi = 3.0, 105.6$ and 225.5 respectively.

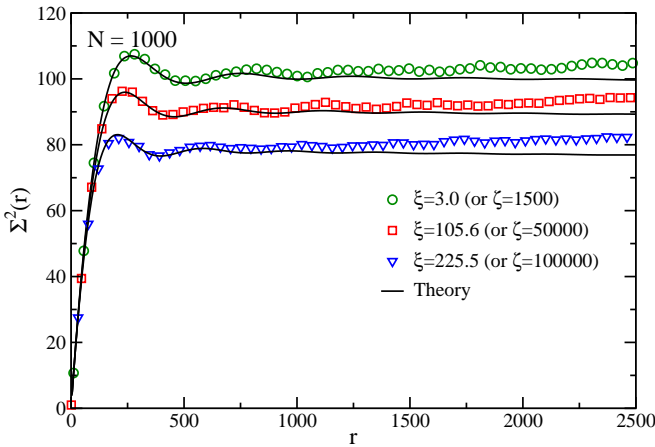


FIG. 7. (Color online) Number variance vs. r for EGUE for three regions denoted by ξ . Solid lines are obtained from (38).

Substituting (42) in (38) and ignoring the lower order terms, we get the saturation value for $r \gtrsim N$,

$$\Sigma_{\text{sat}}^2(r; \xi) = \frac{2}{\pi^2} R_1^{(2)}(\xi), \quad (43)$$

which is same as derived from (31).

X. EMBEDDED GAUSSIAN SYMPLECTIC ENSEMBLE

For the Gaussian symplectic ensemble, the form factor, $b_2(k)$ is given by [3],

$$b_2(k) = \begin{cases} 1 - \frac{1}{2}|k| + \frac{1}{4}|k| \log(|(1 - |k|)|), & |k| < 2, \\ 0, & |k| > 2. \end{cases} \quad (44)$$

By using (21), the two particle form factor can be written as,

$$F_2^{(2)}(k; \xi) = \begin{cases} \left[\frac{|k|}{2} - \frac{|k|}{4} \log(|(1 - |k|)|) \right]^2, & |k| < 2, \\ 1, & |k| > 2, \end{cases} \quad (45)$$

where $\chi = kR_1^{(2)}(\xi)$. We calculate the form factor, $F_2^{(2)}(k; \xi)$ using (27). The numerical results are displayed in Fig.8. We observe good agreement with the analytical expressions given in (45). Note that $F_2^{(2)}$ becomes singular for $|k|R_1^{(2)}(\xi) = 1$ as also does $1 - b_2(k)$ at $|k| = 1$ for the one-particle case in (44).

We evaluate number variance by substituting the form factor for EGSE from (45) in (26). The calculation for evaluating number variance is given in Appendix D. We finally get the following expression for the number variance,

$$\begin{aligned} \Sigma^2(r; \xi) = \frac{R_1^{(2)}(\xi)}{8\pi^2} & \left[14 + 8\pi^2\Delta - \frac{2\cos(2\pi\Delta)\text{Si}(2\pi\Delta)}{\pi\Delta} \right. \\ & - 16\pi\Delta\text{Si}(4\pi\Delta) - 4\cos(4\pi\Delta) - \frac{\sin(4\pi\Delta)}{\pi\Delta} \\ & \left. - 2\cos(2\pi\Delta) {}_2F_3 \left[\begin{matrix} \frac{1}{2}, \frac{1}{2} \\ \frac{3}{2}, \frac{3}{2}, \frac{3}{2} \end{matrix}; -\pi^2\Delta^2 \right] \right]. \quad (46) \end{aligned}$$

Here ${}_2F_3$ represents the hypergeometric function defined as,

$${}_2F_3 \left[\begin{matrix} a_1, a_2 \\ b_1, b_2, b_3 \end{matrix}; x \right] = \sum_{k=0}^{\infty} \frac{(a_1)_k (a_2)_k}{(b_1)_k (b_2)_k (b_3)_k} \frac{x^k}{k!}, \quad (47)$$

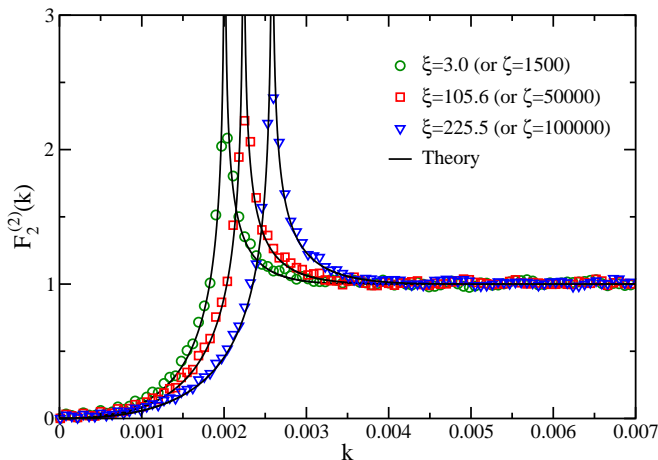


FIG. 8. (Color online) Two particle form factor for the EGSE for three values of ξ .

where $(a)_n$ is the Pochhammer symbol, given by

$$(a)_n = \frac{\Gamma(a+n)}{\Gamma(a)}. \quad (48)$$

The number variance is shown in Fig.9. The numerical results follow the analytical expression very well. Again we consider the $N = 5000$ case in Section XIII for better agreement for large r values.

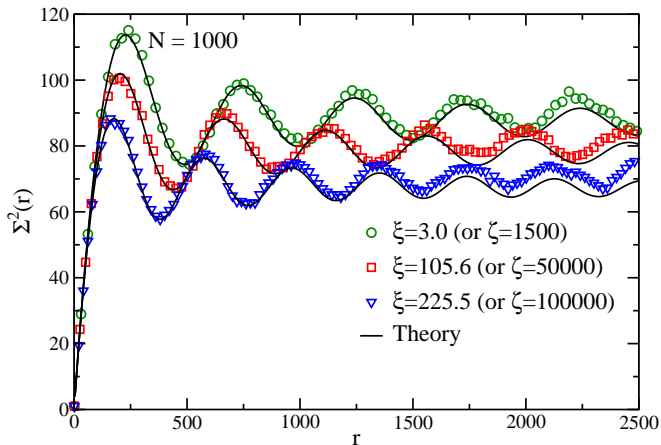


FIG. 9. (Color online) Variation of number variance with r for EGSE. The number variance is calculated for various values of ξ .

Behavior at small correlation lengths is obtained by evaluating the Taylor expansion of the above expression around $r = 0$. The number variance for small r can be written as,

$$\Sigma^2(r; \xi) = R_1^{(2)}(\xi) \left(\Delta - \frac{28}{27} \Delta^2 \dots \right). \quad (49)$$

Substituting (16) in the Taylor expansion, we get,

$$\Sigma^2(r; \xi) = r - \frac{1}{R_1^{(2)}(\xi)} \frac{28}{27} r^2 + \dots \quad (50)$$

Again since $R_1^{(2)}(\xi) = O(N)$, $\Sigma^2(r)$ is linear in r for $r \ll N$. We have shown the linear behavior of number variance for EGSE at small values of r in Fig.2. The saturation value of Σ^2 at large correlation lengths can be obtained by evaluating the limiting values of the higher order terms. Using (42) and ignoring the lower order terms, we get the saturation value, given by

$$\Sigma_{\text{sat}}^2(r, \xi) = \frac{7}{4\pi^2} R_1^{(2)}(\xi) \text{ for } r \approx O(N), \quad (51)$$

again consistent with (31). Note that the hypergeometric function, ${}_2F_3$, converges to zero for large values of r .

XI. EMBEDDED GAUSSIAN ORTHOGONAL ENSEMBLE

We consider the form factor for EGOE. The one particle form factor is given by,

$$b_2(k) = \begin{cases} 1 - 2|k| + |k| \log(1 + 2|k|), & |k| \leq 1, \\ -1 + |k| \log\left(\frac{2|k|+1}{2|k|-1}\right), & |k| \geq 1. \end{cases} \quad (52)$$

Using (23), we have for the two-particle system,

$$F_2^{(2)}(k; \xi) = \begin{cases} [2|\chi| - |\chi| \log(1 + 2|\chi|)]^2, & |\chi| \leq 1, \\ \left[2 - |\chi| \log\left(\frac{2|\chi|+1}{2|\chi|-1}\right)\right]^2, & |\chi| > 1, \end{cases} \quad (53)$$

where $\chi = kR_1^{(2)}(\xi)$. We calculate the two-particle form factor, $F_2^{(2)}(k; \xi)$, using (27). The form factor for EGOE at several values of ξ is shown in Fig.10. The numerical results are in good agreement with the analytical expression given in (53).

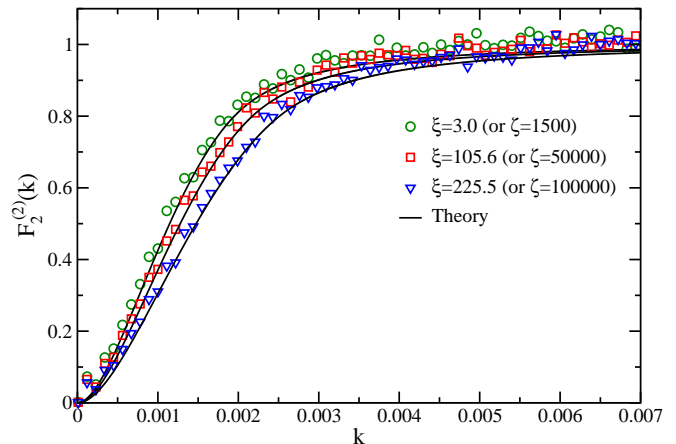


FIG. 10. (Color online) The two particle form factor for EGOE for three values of ξ .

To evaluate the number variance, we substitute the two-particle form factor for EGOE from (53) in (26). The number variance can be written as,

$$\begin{aligned}
\Sigma^2(r; \xi) = & \frac{R_1^{(2)}(\xi)}{2\pi^3 \Delta} \left[\cos(\pi\Delta)[4\text{Si}(\pi\Delta) + (\log 9 - 4)\text{Si}(3\pi\Delta)] - \sin(\pi\Delta)[4\text{Ci}(\pi\Delta) + (\log 9 - 4)\text{Ci}(3\pi\Delta)] \right. \\
& - 2\pi\Delta \cos(2\pi\Delta) - (\log 3 - 2)^2 \sin(2\pi\Delta) + \pi\Delta[22 + 3 \log 3(\log 3 - 6) - 4\pi\Delta\text{Si}(2\pi\Delta)] - \pi \log 3 \cos(\pi\Delta) \\
& \left. + 2\pi^3 \Delta^2 + 2 \int_1^3 \int_\Delta^\infty \frac{\sin(\pi(kt - \Delta))}{kt} dk dt \right] + \sigma, \tag{54}
\end{aligned}$$

where

$$\begin{aligned}
\sigma = & 2R_1^{(2)}(\xi) \int_1^\infty \left[3 + \left[k \log \left(\frac{2k+1}{2k-1} \right) \right]^2 \right. \\
& \left. - 4k \log \left(\frac{2k+1}{2k-1} \right) \right] \left(\frac{\sin(\pi k \Delta)}{\pi k} \right)^2 dk. \tag{55}
\end{aligned}$$

See Appendix E for the derivation of (54). We numerically obtain the number variance for EGOE at several values of ξ . We show in Fig.11 the numerical results and its verification with the analytical expression given in (54). Note that we calculate σ numerically while calculating number variance from (54). Again much better agreement is found for $N = 5000$ as shown in Section XII.

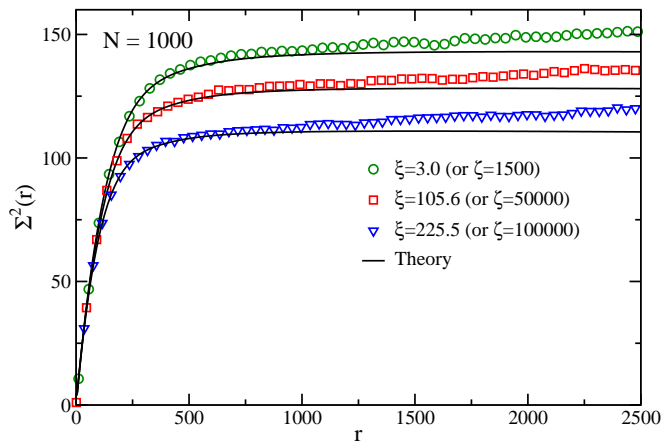


FIG. 11. (Color online) Number variance vs. r for EGOE. The spectra are generated from the one particle spectra of size $N = 1000$. Number variance is evaluated for $\xi = 3.0, 105.6$ and 225.5 .

We calculate the number variance for small correlation lengths in Fig.2. We obtain linear behavior as in the case of EGUE and EGSE.

For number variance at large correlation lengths, we solve (53, 31) directly for large values of Δ . We find,

$$\Sigma_{\text{sat}}^2(r; \xi) = \frac{1}{2\pi^2} [28 - 18 \log(3) - 12\text{Li}_2(-2) - 2\pi^2] R_1^{(2)}(\xi) \tag{56}$$

for $r \approx O(N)$. Here $\text{Li}_2(x) = \sum_{k=1}^\infty x^k/k^2$ is the Dilogarithm function.

XII. NUMBER VARIANCE FOR $N = 5000$

The number variance for all three ensembles, viz., EGOE, EGUE and EGSE at $N = 1000$ show small departures from the theoretical results for larger values of correlation lengths ($r \gtrsim N$). This is a finite- N effect. To improve the agreement, we evaluate the number variance for $N = 5000$ with ensemble having 5000 matrices. We find that the number variance follows the theoretical results for much larger correlation lengths ($r = O(4N)$) as shown in Fig.12.

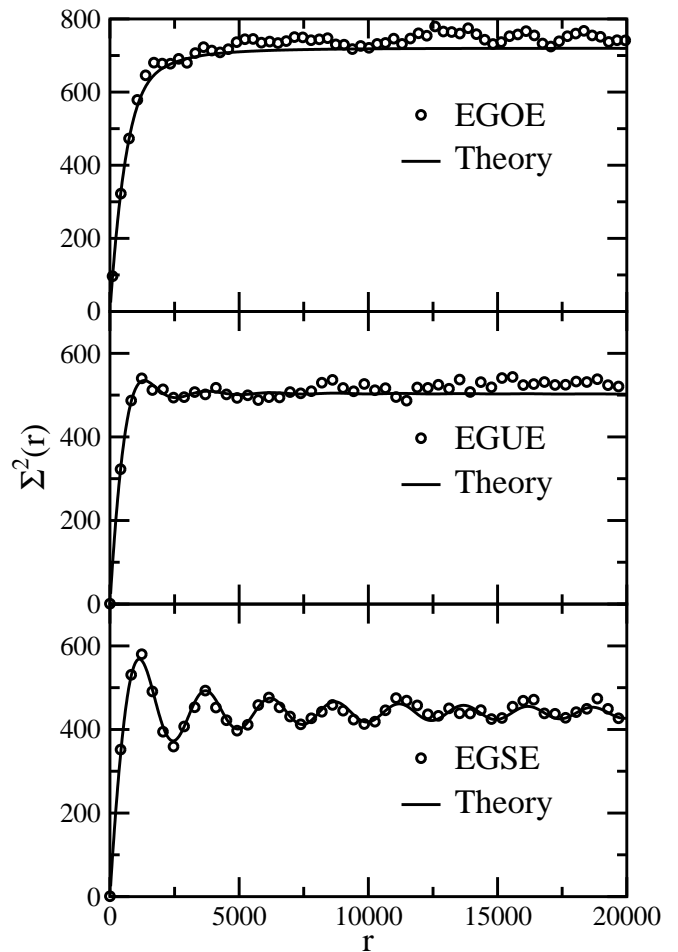


FIG. 12. Number variance for all three ensembles at $N = 5000$ and $\xi = 20.0$, which is equivalent to $\zeta = 50000$.

XIII. SATURATION OF NUMBER VARIANCE FOR NON-UNIFORM DENSITY

We have considered above the number variance for the case when the one-particle spectral density is uniform. We now consider the number variance briefly for the case when the one-particle ensemble is GUE. Thus, the one-particle spectral density is semicircle and is given by

$$R_1(x) = \frac{1}{2\pi} \sqrt{4N - x^2}. \quad (57)$$

We numerically obtain the two-particle density and also numerically unfold it to obtain number variance. The two-particle spectral density and number variance are shown in Fig.13a and Fig.13b respectively. Again we find saturation similar to (31). Note that in both cases the data correspond to the same regions in the unfolded two-particle spectrum viz. $\zeta = 1500, 50000$ and 100000 respectively for upper, middle and lower curves. We see that the saturation phenomenon is universal, but the actual numbers are different.

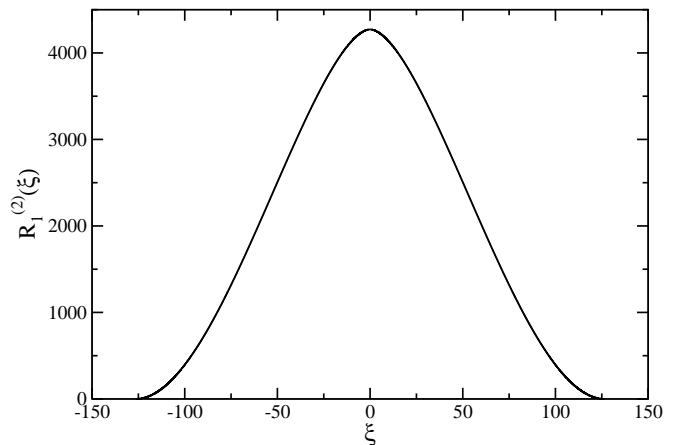
We emphasize that the $R_1^{(2)}$ used in all the expressions for $\Sigma^2, R_2^{(2)}, Y_2^{(2)}$ given in the earlier sections are valid only for the uniform case. The general theory that covers all types of one-particle density is yet to be worked out.

XIV. CONCLUSION

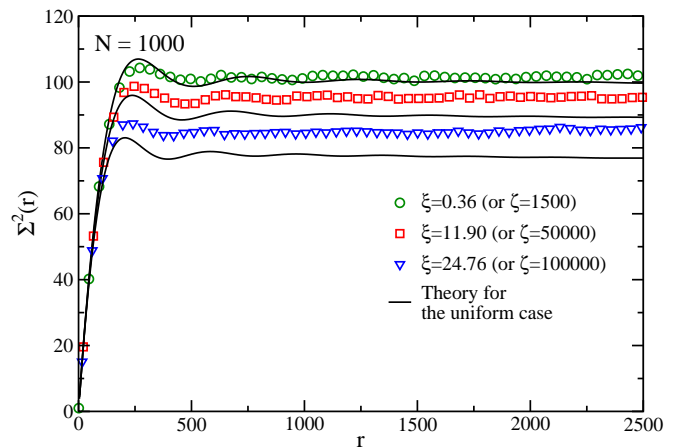
We have studied the embedded ensembles for systems of two non-interacting particles. The one-particle spectra are modeled by (unfolded) Gaussian ensembles. We have derived correlation functions for such systems and studied the local fluctuation properties like nearest neighbor spacing distribution and the number variance. We find that for small correlation lengths two particle spectrum exhibits Poisson statistics which is a key behavior of integrable systems. For higher correlation lengths, the number variance approaches saturation values. We find that saturation (viz., linear to constant transition) occurs due to suppression of fluctuations of short-wave frequencies. Thus, spectra are rigid for such lengths. We study the number variance and their saturation values for all three types of embedded Gaussian ensembles, constructed using the spectrum of Gaussian ensembles viz., GOE, GUE and GSE, as the one-particle spectrum. The saturation phenomenon has been studied for chaotic systems also by semiclassical methods. We present a heuristic model to illustrate the saturation phenomenon in the embedded ensembles of interacting particles. In these cases the spectrum displays a logarithmic to constant transition.

ACKNOWLEDGMENTS

Ravi Prakash acknowledges CSIR, India for financial support.



(a) Spectral density



(b) Number variance

FIG. 13. (Color online) Spectral density and number variance for two-particle spectrum constructed from one-particle spectra with semi-circular spectral density given in (57) with $N = 1000$. Number variance is calculated in the same region on the unfolded scale where it was calculated in Fig. 7. Data points denoted by circle, square and triangle represent the number variance around $\zeta = 1500, 50000$ and 100000 respectively. Upper, middle and lower solid lines represent the number variance in the same region for the uniform case (i.e. for $R_1(x) = 1$).

Appendix A: Correlation function for the two-particle spectrum

The correlation functions can be written in terms of cluster functions using the definition given in (4). One and two-level correlation functions are given in (5) and (6) respectively. Similarly, three and four-level correlation functions can be written as,

$$\begin{aligned} R_3(x_1, x_2, x_3) = & T_3(x_1, x_2, x_3) \\ & - T_1(x_1)T_2(x_2, x_3) - T_1(x_2)T_2(x_1, x_3) \\ & - T_1(x_3)T_2(x_1, x_2) \\ & + T_1(x_1)T_1(x_2)T_1(x_3), \end{aligned} \quad (A1)$$

and

$$\begin{aligned}
R_4(x_1, x_2, x_3, x_4) &= -T_4(x_1, x_2, x_3, x_4) \\
&+ T_1(x_1)T_3(x_2, x_3, x_4) + \dots + \dots \text{(4 terms)} \\
&+ T_2(x_1, x_2)T_2(x_3, x_4) + \dots + \dots \text{(3 terms)} \\
&- T_1(x_1)T_1(x_2)T_2(x_3, x_4) - \dots - \dots \text{(6 terms)} \\
&+ T_1(x_1)T_1(x_2)T_1(x_3)T_1(x_4). \tag{A2}
\end{aligned}$$

Note that the R_n are normalized to $N(N-1)\dots(N-n+1)$. Similarly two-particle correlation function, $R_n^{(2)}$, are normalized to $d_2(d_2-1)\dots(d_2-n+1)$.

We will derive general expression for the spectral density and the two-level correlation function in terms of the correlation functions belonging to the single particle spectrum. The spectral density for the two-particle spectrum, $R_1^{(2)}(\xi)$, is given by

$$\begin{aligned}
R_1^{(2)}(\xi) &= \int_{-\infty}^{\infty} \int_{-\infty}^{\infty} [C_2 R_2(x_1, x_2) + C_1 R_1(x_1) \delta(x_1 - x_2)] \\
&\times \delta(\xi - (x_1 + x_2)) dx_1 dx_2. \tag{A3}
\end{aligned}$$

The values of coefficients C_1 and C_2 in (A3) are determined by the contribution of their corresponding correlation functions to the two particle spectrum. We know that two fermions can not occupy same energy level. Thus, we have, $C_1 = 0$. The normalization values on the left-hand side and right-hand side are $d_2 = N(N-1)/2$ and $C_2 N(N-1)$ respectively. We, therefore, have $C_2 = 1/2$. Substituting these values in (A3), we get,

$$R_1^{(2)}(\xi) = \frac{1}{2} \int_{-\infty}^{\infty} \int_{-\infty}^{\infty} R_2(x_1, x_2) \delta(\xi - (x_1 + x_2)) dx_1 dx_2. \tag{A4}$$

By substituting the relation between the correlation and cluster functions given in (5) and (6), we get the spectral density in terms of the cluster functions as given in (7) of the main text.

The two level correlation function, $R_2^{(2)}$, can be evaluated from the four level and lower-order correlation functions of the one particle spectrum. Thus $R_2^{(2)}$ can be

expressed as a linear function of R_4 and R_3 as follows,

$$\begin{aligned}
R_2^{(2)}(\xi_1, \xi_2) &= \int_{-\infty}^{\infty} \int_{-\infty}^{\infty} \int_{-\infty}^{\infty} \int_{-\infty}^{\infty} [C_4 R_4(x_1, x_2, x_3, x_4) \\
&+ C_3 R_3(x_1, x_2, x_3) R_1(x_4) \delta(x_1 - x_4)] \delta(\xi_1 - (x_1 + x_2)) \\
&\times \delta(\xi_2 - (x_3 + x_4)) dx_1 dx_2 dx_3 dx_4. \tag{A5}
\end{aligned}$$

For Fermions, it can be assumed without any loss of generality that $x_1 > x_2$, $x_3 > x_4$ and $x_1 + x_2 \neq x_3 + x_4$. Under these conditions it can be easily verified that R_2 and R_1 can not contribute. Therefore, these are not considered in (A5). The coefficients C_3 and C_4 are determined by their contributions to the two-particle correlation function. The normalization on left-hand side is equal to $d_2(d_2-1) = (N+1)N(N-1)(N-2)/4$. There are $N(N-1)(N-2)(N-3)/4$ permutations of x_1, x_2, x_3, x_4 such that all four x -variables are different. Therefore, these permutations must be equal to the normalization of $C_4 R_4$. The remaining $N(N-1)(N-2)$ permutations are such that two of the x -variables are same. So these permutations should be equal to the normalization of $C_3 R_3$. To keep the normalization equal to these values, we must have C_4 and C_3 equal to $1/4$ and 1 respectively. Substituting these values in (A5) and putting $R_1(x) = 1$, we get the expression for $R_2^{(2)}$ given in the main text by (8).

Appendix B: Two-level correlation function for the two-particle spectrum

We write $R_2^{(2)}$ as the sum of two functions, I_4 and I_3 , where I_4 is the integral over the R_4 term and I_3 is the integral over the R_3 term given in (8). Thus $R_2^{(2)}$ is given by

$$R_2^{(2)} = \frac{1}{4} I_4 + I_3. \tag{B1}$$

The order of integration of T_3 and T_4 terms is much lower than the remaining terms. We ignore these terms in further calculations.

We first calculate I_4 . We have

$$\begin{aligned}
I_4 &= \int_{-N/2}^{N/2} \int_{-N/2}^{N/2} \int_{-N/2}^{N/2} \int_{-N/2}^{N/2} \left[T_2(x_1, x_4) T_2(x_2, x_3) + T_2(x_1, x_3) T_2(x_2, x_4) - \sum_{i=1}^2 \sum_{j=3}^4 T_2(x_i, x_j) \right] \\
&\times \delta(\xi_1 - (x_1 + x_2)) \delta(\xi_2 - (x_3 + x_4)) dx_1 dx_2 dx_3 dx_4 + 4R_1^{(2)}(\xi_1) R_1^{(2)}(\xi_2). \tag{B2}
\end{aligned}$$

Here we have used (7, 9) in (B2). The integrand in (B2) remains the same if we interchange x_1 with x_2 and x_3 with x_4 . Therefore the first two terms give same values upon integration and the other four terms in the summa-

tion also yield same values. Thus, we get,

$$\begin{aligned}
I_4 &= \int_{-N/2}^{N/2} \int_{-N/2}^{N/2} \int_{-N/2}^{N/2} \int_{-N/2}^{N/2} [2T_2(x_1, x_3) T_2(x_2, x_4) \\
&- 4T_2(x_1, x_3)] \delta(\xi_1 - (x_1 + x_2)) \\
&\times \delta(\xi_2 - (x_3 + x_4)) dx_1 dx_2 dx_3 dx_4 \\
&+ 4R_1^{(2)}(\xi_1) R_1^{(2)}(\xi_2). \tag{B3}
\end{aligned}$$

For $\xi_1, \xi_2 \geq 0$ we find,

$$I_4 = \int_{-N/2+\xi_2}^{N/2} \left(\int_{-N/2+\xi_1}^{N/2} [2T_2(x_1, x_3)T_2(\xi_1 - x_1, \xi_2 - x_3) - 4T_2(x_1, x_3)] dx_1 \right) dx_3 + 4R_1^{(2)}(\xi_1) R_1^{(2)}(\xi_2). \quad (\text{B4})$$

The one-particle cluster functions are translationally invariant for the unfolded spectra. Using (10), I_4 can be written as,

$$I_4 = \int_{-N/2+\xi_2}^{N/2} \left(\int_{-N/2+\xi_1}^{N/2} [2Y_2(x_3 - x_1)Y_2(\Delta - (x_3 - x_1)) - 4Y_2(x_1 - x_3)] dx_1 \right) dx_3 + 4R_1^{(2)}(\xi_1) R_1^{(2)}(\xi_2), \quad (\text{B5})$$

where $\Delta = \xi_2 - \xi_1$ as defined in (14). Away from the tail of the spectrum, using following change of variables,

$$s_1 = x_3 - x_1; \quad s_2 = x_3 + x_1 \quad (\text{B6})$$

we can simplify (B5) considerably. We find,

$$I_4 = 2(N - \xi) \int_{-\infty}^{\infty} Y_2(s_1)Y_2(\Delta - s_1) ds_1 - 4(N - \xi) + 4R_1^{(2)}(\xi_1) R_1^{(2)}(\xi_2), \quad (\text{B7})$$

where $|\Delta| = O(1)$ and $\xi = (\xi_1 + \xi_2)/2$ as mentioned in (14).

Ignoring T_3 term, we can write I_3 as,

$$I_3 = \int_{-N/2}^{N/2} \int_{-N/2}^{N/2} \int_{-N/2}^{N/2} \int_{-N/2}^{N/2} [1 - T_2(x_1, x_2) - T_2(x_1, x_3) - T_2(x_2, x_3)] \delta(x_1 - x_4) \delta(\xi_1 - (x_1 + x_2)) \times \delta(\xi_2 - (x_3 + x_4)) dx_1 dx_2 dx_3 dx_4.$$

simplifying as above, we find

$$I_3 = \int_{-N/2+\xi_2}^{N/2} [1 - Y_2(2x - \xi_1) - Y_2(2x - \xi_2) - Y_2(\Delta)] dx, \quad (\text{B8})$$

and therefore for large N , we get,

$$I_3 = (N - \xi + \frac{\Delta}{2}) [1 - Y_2(\Delta)]. \quad (\text{B9})$$

Substituting expressions for I_4 and I_3 in (B1) and ignoring terms of $O(1)$, we get,

$$R_2^{(2)}(\xi_1, \xi_2) - R_1^{(2)}(\xi_1) R_1^{(2)}(\xi_2) = \frac{N - |\xi|}{2} \left[\int_{-\infty}^{\infty} Y_2(x)Y_2(\Delta - x) dx - 2Y_2(\Delta) \right]. \quad (\text{B10})$$

This gives the cluster function for two-particle spectrum mentioned in (13) of the main text. Note that the evaluation of (B3) for $\xi_1, \xi_2 \leq 0$ also yields the same result. We have put $|\xi|$ in (B10) to include this case.

Appendix C: Number variance for EGUE

To evaluate the number variance, we substitute the expression for the form factor given in (37) in (26). We get

$$\Sigma^2(r; \xi) = 2 \int_0^{1/R_1^{(2)}(\xi)} [kR_1^{(2)}(\xi)]^2 \left(\frac{\sin(\pi kr)}{\pi k} \right)^2 dk + 2 \int_{1/R_1^{(2)}(\xi)}^{\infty} \left(\frac{\sin(\pi kr)}{\pi k} \right)^2 dk. \quad (\text{C1})$$

Eq.(C1) can be written as,

$$\Sigma^2(r; \xi) = 2R_1^{(2)}(\xi) \int_0^1 k^2 \left(\frac{\sin(\pi k \Delta)}{\pi k} \right)^2 dk + 2R_1^{(2)}(\xi) \int_1^{\infty} \left(\frac{\sin(\pi k \Delta)}{\pi k} \right)^2 dk, \quad (\text{C2})$$

where $r = R_1^{(2)}(\xi)\Delta$ as mentioned in (16). Note that,

$$\int_x^{\infty} \left(\frac{\sin(s)}{s} \right)^2 ds = \frac{(\sin(x))^2}{x} + \frac{\pi}{2} - \int_0^{2x} \frac{\sin(s)}{s} ds. \quad (\text{C3})$$

By substituting (C3) in (C2) we get the number variance given in (38) of the main text.

Appendix D: Number variance for EGSE

We use the form factor for EGSE given in (45) and substitute in (26) to calculate the number variance. We get,

$$\begin{aligned} \Sigma^2(r; \xi) = & 2R_1^{(2)}(\xi) \left[\int_0^1 \left[\frac{|k|}{2} - \frac{|k|}{4} \log(1 - |k|) \right]^2 \left(\frac{\sin(\pi k \Delta)}{\pi k} \right)^2 dk + \int_1^2 \left[\frac{|k|}{2} - \frac{|k|}{4} \log(|k| - 1) \right]^2 \left(\frac{\sin(\pi k \Delta)}{\pi k} \right)^2 dk \right. \\ & \left. + \int_2^\infty \left(\frac{\sin(\pi k \Delta)}{\pi k} \right)^2 dk \right], \end{aligned} \quad (\text{D1})$$

where Δ is related to r as in (16). We regroup and perform suitable transformations of variables to get,

$$\begin{aligned} \Sigma^2(r; \xi) = & \frac{R_1^{(2)}(\xi)}{2\pi^2} \int_0^2 [\sin(\pi k \Delta)]^2 dk \\ & + \frac{2R_1^{(2)}(\xi)}{\pi} \int_{2\pi\Delta}^\infty \left[\frac{\sin(k)}{k} \right]^2 dk \\ & - \frac{R_1^{(2)}(\xi)}{2\pi^2} \int_0^1 \log(k) [1 - \cos(2\pi\Delta) \cos(2\pi\Delta k)] dk \\ & + \frac{R_1^{(2)}(\xi)}{8\pi^2} \int_0^1 [\log(k)]^2 [1 - \cos(2\pi\Delta) \cos(2\pi\Delta k)] dk. \end{aligned} \quad (\text{D2})$$

We mention the following standard integrals,

$$\int_0^1 \log(t) \cos(at) dt = -\frac{\text{Si}(a)}{a}, \quad (\text{D3})$$

$$\int_0^1 [\log(t)]^2 \cos(at) dt = 2 {}_2F_3 \left[\begin{matrix} \frac{1}{2}, \frac{1}{2} \\ \frac{3}{2}, \frac{3}{2}, \frac{3}{2} \end{matrix}; -\frac{a^2}{4} \right], \quad (\text{D4})$$

$$(\text{D5})$$

and

$$\int_0^1 \left[\frac{1}{4} (\log(t))^2 - \log(t) \right] dt = \frac{3}{2}. \quad (\text{D6})$$

Here ${}_2F_3$ represents the hypergeometric function defined by (47,48). We solve (D2) using these expressions to get the number variance given in (46) of the main text.

Appendix E: Number variance for EGOE

The number variance is evaluated by substituting the two-particle form factor for EGOE from (53) in (26). We

get,

$$\begin{aligned} \Sigma^2(r; \xi) = & 2R_1^{(2)}(\xi) \int_0^1 [2|k| - |k| \log(1 + 2|k|)]^2 \\ & \times \left(\frac{\sin(\pi k \Delta)}{\pi k} \right)^2 dk \\ & + 2R_1^{(2)}(\xi) \int_1^\infty \left(\frac{\sin(\pi k \Delta)}{\pi k} \right)^2 dk \\ & + \sigma, \end{aligned} \quad (\text{E1})$$

where σ is given in (55). The integrals involved in (55) are not easy. By numerical calculations, we find that the contribution from (55) is of much lower order. Ignoring the contribution from σ , we get an error of about 6%. Therefore, we solve here (E1) without evaluating the σ term. We take help of the following integrals in solving (E1),

$$\int \log(x) \sin(ax) dx = \frac{\text{Ci}(ax)}{ax} - \frac{\log(x) \cos(ax)}{a}, \quad (\text{E2})$$

$$\int \log(x) \cos(ax) dx = \frac{\log(x) \sin(ax)}{a} - \frac{\text{Si}(ax)}{ax}, \quad (\text{E3})$$

$$\int [\log(x)]^2 dx = 2x - 2x \log(x) + x[\log(x)]^2, \quad (\text{E4})$$

$$\begin{aligned} \int [\log(x)]^2 \sin(ax) dx = & -[\log(x)]^2 \frac{\cos(ax)}{a} \\ & + \frac{2 \log(x)}{a} \text{Ci}(ax) - \frac{2}{a} \int \frac{\text{Ci}(ax)}{x} dx, \end{aligned} \quad (\text{E5})$$

$$\begin{aligned} \int [\log(x)]^2 \cos(ax) dx = & [\log(x)]^2 \frac{\sin(ax)}{a} \\ & - \frac{2 \log(x)}{a} \text{Si}(ax) + \frac{2}{a} \int \frac{\text{Si}(ax)}{x} dx, \end{aligned} \quad (\text{E6})$$

and

$$\int_{a/\pi}^\infty \frac{\sin(\pi s x - a)}{s x} ds = \frac{\text{Ci}(ax) \sin(a)}{x} - \frac{\text{Si}(ax) \cos(a)}{x}. \quad (\text{E7})$$

By substituting the above expressions in (E1), we get the number variance given in (54) of the main text.

-
- [1] E. P. Wigner, *SIAM Rev.* **9**, 1 (1967).
- [2] T. A. Brody, J. Flores, J. B. French, P. A. Mello, A. Pandey, and S. S. M. Wong, *Rev. Mod. Phys.* **53**, 385 (1981).
- [3] M. L. Mehta, *Random Matrices*, Pure and Applied Mathematics, Vol. 142 (Elsevier Science, Amsterdam, 2004).
- [4] O. Bohigas and M.-J. Giannoni, in *Mathematical and Computational Methods in Nuclear Physics*, Lect. Notes Phys., Vol. 209, edited by J. Dehesa, J. Gomez, and A. Polls (Springer, Berlin Heidelberg, 1984) pp. 1–99.
- [5] C. W. J. Beenakker, *Rev. Mod. Phys.* **69**, 731 (1997).
- [6] K. Efetov, *Supersymmetry in Disorder and Chaos* (Cambridge University Press, UK, 1999).
- [7] T. Guhr, A. Müller–Groeling, and H. A. Weidenmüller, *Phys. Rep.* **299**, 189 (1998).
- [8] H. Stöckmann, *Quantum Chaos: An Introduction* (Cambridge University Press, UK, 2006).
- [9] F. Haake, *Quantum Signatures of Chaos*, Physics and astronomy online library (Springer, New York, 2001).
- [10] P. Forrester, *Log-Gases and Random Matrices*, London Mathematical Society Monographs (Princeton University Press, New Jersey, 2010).
- [11] G. Akemann, J. Baik, and P. D. Francesco, *The Oxford Handbook of Random Matrix Theory* (Oxford University Press, New York, 2011).
- [12] Vinayak and A. Pandey, *Phys. Rev. E* **81**, 036202 (2010).
- [13] L. Laloux, P. Cizeau, J.-P. Bouchaud, and M. Potters, *Phys. Rev. Lett.* **83**, 1467 (1999).
- [14] V. Plerou, P. Gopikrishnan, B. Rosenow, L. A. Nunes Amaral, and H. E. Stanley, *Phys. Rev. Lett.* **83**, 1471 (1999).
- [15] S. Kumar and A. Pandey, *IEEE Trans. Inf. Theory* **56**, 2360 (2010).
- [16] A. M. Tulino and S. Verdú, *Found. Trends Commun. Inf. Theory* **1**, 1 (2004).
- [17] M. V. Berry and M. Tabor, *Proc. R. Soc. Lond. A* **356**, 375 (1977).
- [18] R. U. Haq, A. Pandey, and O. Bohigas, *Phys. Rev. Lett.* **48**, 1086 (1982).
- [19] O. Bohigas, M. J. Giannoni, and C. Schmit, *Phys. Rev. Lett.* **52**, 1 (1984).
- [20] M. V. Berry, *Proc. R. Soc. Lond. A* **400**, 229 (1985).
- [21] G. Casati, B. V. Chirikov, and I. Guarneri, *Phys. Rev. Lett.* **54**, 1350 (1985).
- [22] M. V. Berry, *Nonlinearity* **1**, 399 (1988).
- [23] M. V. Berry and J. P. Keating, *SIAM Rev.* **41**, 236 (1999), <http://dx.doi.org/10.1137/S0036144598347497>.
- [24] J. B. French and S. S. M. Wong, *Phys. Lett. B* **33**, 449 (1970).
- [25] O. Bohigas and J. Flores, *Phys. Lett. B* **34**, 261 (1971).
- [26] S. Wong and J. French, *Nucl. Phys. A* **198**, 188 (1972).
- [27] K. K. Mon and J. B. French, *Ann. Phys.* **95**, 90 (1975).
- [28] V. K. B. Kota, *Embedded Random Matrix Ensembles in Quantum Ph* Lecture Notes in Physics, Vol. 884 (Springer, New York, 2014).
- [29] A. Pandey, in *Quantum Chaos and Statistical Nuclear Physics*, Lecture Notes in Physics, Vol. 263, edited by T. Seligman and H. Nishioka (Springer, Berlin Heidelberg, 1986) pp. 98–109.
- [30] Section I.D and IV.F of [2].
- [31] F. J. Dyson, *J. Math. Phys.* **3**, 166 (1962).
- [32] A. Pandey, *Ann. Phys.* **119**, 170 (1979).
- [33] E. Brézin and S. Hikami, *Phys. Rev. E* **55**, 4067 (1997).
- [34] F. J. Dyson and M. L. Mehta, *J. Math. Phys.* **4**, 701 (1963).